1-1-1990

Intrinsic tryptophan fluorescence measurements suggest that polylactosaminyl glycosylation affects the protein conformation of the gelatin-binding domain from human placental fibronectin

Betty C.R. ZHU
Louisiana State University

Roger A. LAINE
Louisiana State University

Mary D. BARKLEY
Louisiana State University

Recommended Citation

ZHU, B., LAINE, R., & BARKLEY, M. (1990). Intrinsic tryptophan fluorescence measurements suggest that polylactosaminyl glycosylation affects the protein conformation of the gelatin-binding domain from human placental fibronectin. *European Journal of Biochemistry, 189* (3), 509-516. https://doi.org/10.1111/j.1432-1033.1990.tb15516.x

Eur. J. Biochem. *189*, 509–516 (1990)

Intrinsic tryptophan fluorescence measurements suggest that polylactosaminyl glycosylation affects the protein conformation of the gelatin-binding domain from human placental fibronectin

Betty C. R. ZHU[1], Roger A. LAINE[2] and Mary D. BARKLEY[3]

Departments of [1, 2] Biochemistry and [2, 3] Chemistry, Louisiana State University, Baton Rouge, Louisiana, USA

Received September 11/November 30, 1989) – EJB 891104

Glycosylation can affect the physical and biochemical properties of the polypeptide chain in glycoproteins. Asparagine-*N*-linked polylactosaminyl glycosylation of the chymotryptic 44-kDa gelatin-binding domain from human placental fibronectin confers protease resistance [Zhu, B. C. R., Fisher, S. F., Panda, H., Calaycay, J., Shively, J. E. & Laine, R. A. (1984) *J. Biol. Chem. 259*, 3962–3970] and weakens the binding to gelatin [Zhu, B. C. R. & Laine, R. A. (1985) *J. Biol. Chem. 260*, 4041–4045]. Intrinsic tryptophan fluorescence of the gelatin-binding domain was used to probe glycosylation-dependent protein conformation changes. In gelatin-binding fragments containing incrementally smaller polylactosamine oligosaccharides, the fluorescence intensity progressively decreased and the emission spectrum shifted about 7 nm to the blue. Removal of the polylactosamine chains from a highly glycosylated fragment with endo-β-galactosidase from *Escherichia freundii* also quenched the protein fluorescence. The fluorescence lifetimes did not appear to be affected by the extent of glycosylation, suggesting static quenching of the tryptophan emission in the low glycosylated fragments. Acrylamide quenching studies showed that the accessibility of the tryptophans to small solutes was not altered by glycosylation. The steady-state emission anisotropy increased with decreasing polylactosamine chain length. The results indicate that the polylactosamine chains alter the tryptophan environments in the gelatin-binding domain, probably by changing the polypeptide conformation. These putative protein conformation changes may be partially responsible for the altered gelatin binding, protease resistance, and cell adhesion functions of fetal tissue fibronectin.

Among other possible sequence-dependent biological functions of carbohydrates, N- and O-linked glycosylation provide a mechanism for modulating protein function. *N*-Asparaginyl-linked carbohydrate chains can modify the functional properties of the polypeptide to which they are attached [1–4]. It has been known for many years that protein *N*-glycosylation is often heterogeneous with respect to the occupancy of glycosylation sites as well as the structural subclasses of carbohydrate occupying a given site. Only recently has it been appreciated that the distinct protein-carbohydrate molecular forms produced by this heterogeneity may serve some purpose. The glycoforms of a glycoprotein comprise a set of identical polypeptides differing in glycosylation [5]. Glycoforms of a single polypeptide may have different biochemical properties. This is particularly true when the carbohydrate chain affects the folded conformation of the polypeptide chain or blocks important regions such as proteolytic cleavage, functional binding, and catalytic sites.

Numerous studies have been performed showing different biochemical, immunological, and physical characteristics of glycoproteins after laboratory modification of naturally occurring carbohydrate chains [6–15]. However, very little is known about the structural and functional attributes of individual glycoforms of naturally occurring glycoproteins, in part because of the difficulty of isolating them. Two glycoforms of α_1-acid glycoprotein have been fractionated on concanavalin-A–Sepharose: one with all five N-linked chains of the biantennary complex type, and the other with a mixture of triantennary and tetraantennary types [16]. The solution conformational properties of these homotypic glycoforms are quite different, though distinct functional roles are as yet unknown [17]. In a few glycoproteins it has been possible to show that individual glycoforms have different biochemical properties. Peterson and Blackburn [3] isolated an antithrombin III glycosylation idiotype which is missing one of four N-linked biantennary complex oligosaccharides. This antithrombin III glycoform binds more tightly to heparin and reacts faster with thrombin than the native inhibitor. However, protein conformation changes could not be detected between the two antithrombin III glycoforms. In homotropic neural cell adhesion molecules, the early embryonic glycoforms have more extended chains of (2–8)-linked poly(sialic acid) and slower binding kinetics than the later embryonic and adult glycoforms [18–20]. No physical studies of the polysialylated glycoforms have been reported.

Previously, we found that the binding of human placental fibronectin to collagen was weakened in glycoforms with extended polylactosamine substitution on the N-linked carbohydrates [4]. This polylactosaminylation is modified steadily

Correspondence to R. A. Laine, Department of Biochemistry, Louisiana State University, Baton Rouge, Louisiana, 70803 USA

Abbreviation. GB44, the chymotryptic 44-kDa gelatin-binding domain of human placental fibronectin.

Enzymes. Chymotrypsin (EC 3.4.21.1); endo-β-galactosidase (EC 3.2.1.103).

throughout gestation, an interesting fact suggesting a programmed glycosylation-dependent functional change in placental fibronectin during pregnancy [21]. The range of polymerization in the polylactosamine chains produces a larger number of glycoforms than other systems, and consequently greater potential for altering protein function. The polylactosamine chains also protect fibronectin against proteolysis [22], in concord with other observations of mitigated protease susceptibility due to the presence of N-linked carbohydrates [6, 23, 24]. Protease protection seems to be one generally accepted purpose of N-linked chains.

In this paper, we use intrinsic tryptophan fluorescence as a probe of protein conformation in the chymotryptic 44-kDa *gelatin-binding domain* of human placental fibronectin (GB44; Ala260–Trp599). A series of GB44 glycoforms was isolated, differing chiefly in the extent of polymerization of polylactosamine on the three N-linked mannose cores [4, 22]. These naturally occurring glycoforms of GB44 were previously shown to have differential protease susecptibility and gelatin-binding affinity. The effects of polylactosamine chain length on the tryptophan emission of GB44 were investigated by fluorescence decay, solute quenching, and emission anisotropy measurements.

MATERIALS AND METHODS

Materials

Endo-β-galactosidase from *E. freundii* was a generous gift from Drs Y. T. Li and S. C. Li (Tulane University Medical Center). Chymotrypsin (treated with tosyllysylchloromethane), gelatin (type I, swine skin), phenylmethylsulfonyl fluoride, and *N*-acetyltryptophanamide were obtained from Sigma. Sepharose 4B and 6B and Sephadex G-25 and G-200 were from Pharmacia. Ultra-pure urea and acrylamide were purchased from Schwarz/Mann Biotech. Other reagents were analytical grade.

Preparation of GB44

Human placental fibronectin was purified from fresh placenta by affinity chromatography on gelatin–Sepharose 4B [22]. The gelatin-binding fragment GB44 was isolated by affinity chromatography on gelatin–Sepharose 4B after digestion of intact fibronectin (1 mg/ml) with chymotrypsin (20μg/ml) at room temperature for 60 min. Glycoforms of the gelatin-binding fragment were fractionated by gel permeation chromatography on Sephadex G-200 in 20 mM phosphate pH 7.0 at 4°C [4]. The Sephadex G-200 column was calibrated with blue dextran (2000 kDa), bovine serum albumin (66 kDa) and ovalbumin (45 kDa). The glycoforms were eluted in the fractions between bovine serum albumin and ovalbumin. For the control experiment polylactosamine chains were removed from a high-polylactosamine glycoform (0.2 mg/ml) by digestion with endo-β-galactosidase (0.2 μg/ml) at 37°C for 48 h [22] followed by affinity chromatography on a gelatin–Sepharose 4B column eluted with 4 M urea. The endo-β-galactosidase-treated glycoform was chromatographed on Sephadex G-200 as described above and was eluted in the same fractions as ovalbumin. Protein concentration was determined by amino acid analysis. All glycoprotein samples were dialyzed into 20 mM phosphate pH 7.0 and clarified by centrifugation prior to spectroscopic measurements.

Steady-state measurements

Absorbance was measured in a Spectronic 2000 spectrophotometer. Fluorescence was measured at 22°C in a SLM 8000 spectrofluorometer interfaced to an Apple II+ microcomputer. The excitation wavelength was 295 nm (4-nm bandpass) to avoid exciting tyrosine residues. The protein absorbance at 295 nm was 0.1 with a 4-mm path length. Fluorescence emission (16-nm bandpass) was measured in the ratio mode and background fluorescence from a solvent blank was subtracted. Emission spectra were corrected for wavelength-dependent instrument response. Spectral and quenching measurements were made with the excitation and emission polarizers set at 55° and 0°, respectively, to eliminate anisotropic effects.

Fluorescence quantum yields were determined relative to quinine sulfate (Eastman) by dissolving a crystal in 0.5 M H_2SO_4 (double-distilled, GFS Chemicals) and adjusting the absorbance at 350 nm to < 0.1. Sample yields were calculated assuming a value of 0.550 for quinine sulfate at 22°C [25].

Fluorescence quenching experiments were done by adding small aliquots of 1, 2, or 8 M stock solutions of acrylamide in water. Intensities were acquired for five 10-s time intervals and the values were averaged. The quenching data were analyzed according to the modified Stern-Volmer equation,

$$\frac{I_o}{\Delta I} = \frac{1}{f_a} + \frac{1}{f_a K_{sv}[Q]}$$

where $\Delta I = I_o - I$, I_o and I are the intensities in the absence and presence of quencher Q, f_a is the fraction of emission accessible to quencher, and K_{sv} is the Stern-Volmer constant. The values of f_a and K_{sv} were obtained by linear regression.

Fluorescence polarization data were acquired for five 10-s time intervals and the values were averaged. The emission anisotropy $\langle r \rangle$ was calculated from

$$\langle r \rangle = (I_{vv} - GI_{vh})/(I_{vv} + 2GI_{vh}),$$

where the first and second subscripts refer to the orientation of the excitation and emission polarizers, respectively ($v = 0°$; $h = 90°$), and $G = I_{hv}/I_{hh}$ is an instrumental correction factor.

Time-resolved fluorescence measurements

Fluorescence lifetimes were measured at 10°C in a Photochemical Research Associates nanosecond fluorometer with a T optical design. The flash lamp was filled with 170 kPa N_2 and operated at 20–25 kHz with 5 kV applied across a 1.5-mm electrode gap. Under these conditions the pulse width was about 1.7 ns fwhm. Excitation at 296 nm was selected by a microCoatings (Westford, MA) interference filter (10-nm bandpass). Since the incident light was unpolarized, a single polarizer oriented at 35° was used on the emission side to eliminate anisotropic effects. Emission wavelengths were selected by Instruments SA H-10 monochromators (16-nm bandpass). Fluorescence decays were acquired by alternating between a fluorescent sample and a reference fluorophore for the instrument response. The sample decay curve contained about 10^4 counts in the peak channel. Decay curves were stored in 512 channels of 0.108 ns/channel. Data acquisition was controlled by a Digital Equipment Corporation MINC-11 computer. A solution of terphenyl (Aldrich Chemical Co.) in 75% ethanol, 0.8 M KI (containing a trace of thiosulfate to retard I_3^- formation) was used as the reference fluorophore. A lifetime of 0.25 ns for the quenched terphenyl was determined in separate experiments using *N*-acetyltryptophan-

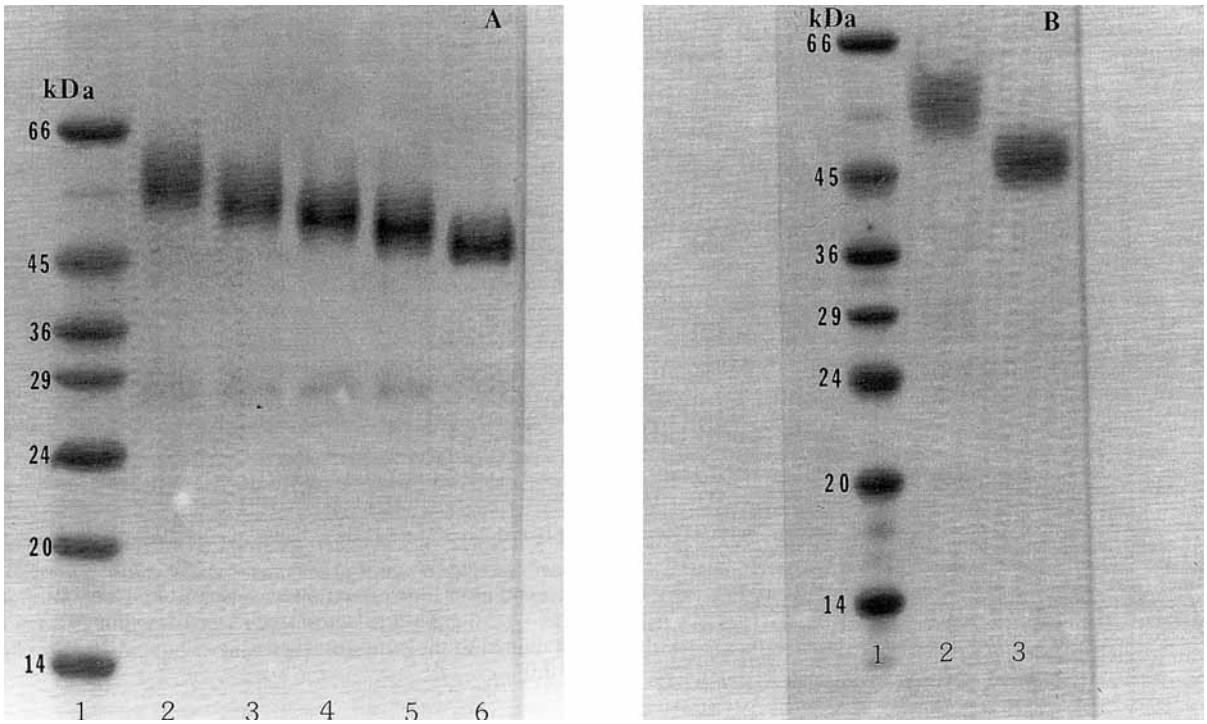

Fig. 1. *SDS/polyacrylamide gel electrophoresis of GB44 fragments.* Coomassie-blue-stained gels of: (A) fractions 29, 31, 33, 35, and 37 from Sephadex G-200 column (lanes 2–5) and (B) fraction 29 incubated in the absence (lane 2) and presence (lane 3) of endo-β-galactosidase. Lane 1 contains molecular mass standards: bovine serum albumin, 66 kDa; ovalbumin, 45 kDa; glyceraldehyde-3-phosphate dehydrogenase, 36 kDa; carbonic anhydrase, 29 kDa; trypsinogen, 24 kDa, α-lactalbumin, 14 kDa

amide in phosphate-buffered saline as the monoexponential standard.

Fluorescence decay data were fitted by reference deconvolution to a sum of exponentials plus a term for scattered light [26],

$$I(\lambda,t) = \Sigma_i \alpha_i(\lambda) \exp(-t/\tau_i) + a(\lambda)\delta(t),$$

where $\alpha_i(\lambda)$ is the amplitude at wavelength λ and τ_i is the fluorescence lifetime for component i, $a(\lambda)$ is the amount of light scattered at wavelength λ, and $\delta(t)$ is the delta function. Goodness of fit was evaluated from the value of reduced χ_r^2 and the shape of the autocorrelation function of the weighted residuals. The reference lifetime was an adjustable parameter in analyses of the monoexponential standard. Its value was fixed at 0.25 ns in analyses of protein samples. Fluorescence decay curves acquired at different emission wavelengths were deconvolved by single-curve analysis and by multiple-curve analysis in a global program [27]. The global analysis assumes that the lifetimes but not the amplitudes and scattered light are independent of emission wavelength.

Decay-associated emission spectra $I_i(\lambda)$ were calculated by scaling the fractional intensities $f_i(\lambda)$ from the time-resolved spectral data to the corrected steady-state emission spectrum $I(\lambda)$,

$$I_i(\lambda) = f_i(\lambda) I(\lambda).$$

The fractional contribution $f_i(\lambda)$ of component i to the fluorescence intensity at wavelength λ is

$$f_i(\lambda) = \alpha_i(\lambda)\tau_i / \Sigma_i \alpha_i(\lambda)\tau_i.$$

The above equation neglects the contribution of scattered light to the total intensity. This is justified because stray light rejection is better in the steady-state instrument than in the nanosecond instrument. The centers of gravity $\nu_{cg,i}$ (in nm^{-1}) of the decay-associated spectra were calculated from [28]

$$\nu_{cg,i} = \Sigma_j I_i(\lambda_j)\lambda_j^{-3} / \Sigma_j I_i(\lambda_j)\lambda^{-2},$$

where the wavelength λ_j increases from 320 nm to 370 nm in 10-nm intervals.

RESULTS

Emission spectra of GB44 glycoforms

Chromatography of GB44 on Sephadex G-200 resulted in separation of a series of glycoforms of the same polypeptide [4, 22]. SDS/polyacrylamide gel electrophoresis of fractions collected across the peak showed that the apparent molecular mass ranged from about 58 kDa for fraction 29 to 46 kDa for fraction 37 (Fig. 1 A). The glycoprotein bands on the gel are wider than the molecular mass markers, probably due to heterogeneity in carbohydrate chain length. Table 1 gives the approximate molecular mass distribution of individual fractions from the Sephadex G-200 column. The glycopeptides from these fractions were previously characterized [4, 22]. The glycopeptides are identical and the carbohydrates consist of the three N-linked complex-type chains with linear lactosamine oligomers chiefly terminated in sialic acid. The higher-molecular-mass glycoforms contain polylactosamine and the lower-molecular-mass glycoforms contain either single lactosamine-type or very short oligolactosamine-type complex structures.

The absorption spectrum of the polypeptide was not affected by the extent of glycosylation of GB44 (not shown). However, the intrinsic trptophan fluorescence of GB44 was sensitive to glycosylation. Fig. 2 shows that the fluorescence inten-

Table 1. *Steady-state fluorescence of GB44 glycoforms*
Molecular mass was estimated from the data in Fig. 1 A. Anisotropy was determined at 295 nm excitation wavelength, 350 nm emission wavelength

Fraction	Molecular mass	λ_{max}	Quantum yield	Anisotropy
	kDa	nm		
29	54–62	349	0.0171	0.068
31	50–60	344	–	0.098
33	47–56	344	–	0.120
35	46–54	342	–	0.138
37	42–50	342	0.0087	0.145

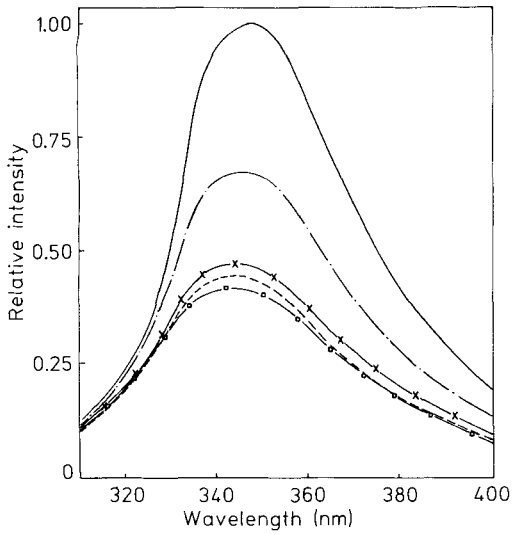

Fig. 2. *Fluorescence emission spectra of GB44 glycoforms.* Fractions from the Sephadex G-200 column were dialyzed and diluted to the same absorbance (0.25) at 280 nm in 20 mM phosphate pH 7.0. Emission spectra of samples measured at 295 nm excitation wavelength, 22 °C: (——) fraction 29, (– · – · –) fraction 31, (×——×) fraction 33, (– – – –) fraction 35, and (□——□) fraction 37

sity drops and the emission maximum shifts slightly to the blue with decreasing lactosamine chain length. The protein concentrations of these samples, as determined by amino acid analysis, were the same within experimental error (5.7 ± 0.3 μM). Fraction 31, which contains 4–5-kDa saccharide chains, had about 70% of the intensity of fraction 29, which contains 5–6.5-kDa chains. The intensities of fractions 33, 35, and 37, which contain 2–3-kDa saccharide chains, were only about 50% relative to fraction 29. The emission maximum shifted from about 349 nm in fraction 29 to 342 nm in fraction 37 (Table 1). The fluorescence emission of indole, the chromophore of tryptophan, is highly sensitive to solvent polarity, with a maximum at about 347 nm in water compared to 298 nm in hexane [29]. The emission maxima of the GB44 glycoforms indicate that the tryptophans are in polar environments in the glycoprotein. The fluorescence quantum yields of the glycoforms are low (Table 1). The emission maximum and quantum yield of fraction 37 are similar to the values reported by Isaacs et al. [30] for the thermolytic 42-kDa gelatin-binding domain from human plasma fibronectin. The polypeptides of the gelatin-binding fragments isolated by thermolysin digestion of plasma fibronectin and by

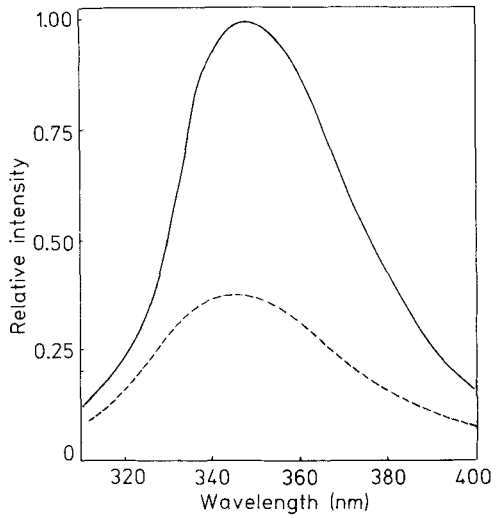

Fig. 3. *Fluorescence emission spectrum of high-molecular-mass GB44 glycoform after removal of polylactosamine chains.* Emission spectra measured at 295 nm excitation wavelength, 22 °C; (——) fraction 29 and (– – – –) endo-β-galactosidase-treated fraction 29 were dialyzed and diluted to the same absorbance at 280 nm in 20 mM phosphate, pH 7.0

chymotrypsin digestion of placental fibronectin are identical except for a few amino acid differences at the N- and C-termini. Both glycoproteins contain N-linked complex-type carbohydrates: the plasma glycoform has two biantennary chains with a single lactosamine, whereas fraction 37 has three bi- and tetraantennary chains with one or a few lactosamines [4].

The polylactosamine chains were removed from fraction 29 by digestion with endo-β-galactosidase, which cleaves at internal galactose residues linked to glucosamine and releases GlcNAcβ1-3Gal disaccharides. The deglycosylated protein eluted from the Sephadex G-200 column at about the same volume as fraction 37. SDS/polyacrylamide gel electrophoresis shows the decrease in apparent molecular mass of fraction 29 treated with endo-β-galactosidase and condensation of the band due to removal of polylactosamine sequences from the glycopeptide (Fig. 1 B). The fluorescence intensity of fraction 29 dropped to about 40% of its original value and the emission maximum shifted about 7 nm to the blue after digestion with endo-β-galactosidase (Fig. 3). These results confirm that the differences in intrinsic fluorescence of the various glycoforms are induced by the carbohydrate moiety. The effects of carbohydrate chain length on the tryptophan emission of GB44 were further characterized by fluorescence lifetime, acrylamide quenching, and anisotropy measurements on the high- and low-molecular-mass glycoforms.

Fluorescence lifetimes

Fluorescence decay curves were acquired for fractions 29 and 37 at six emission wavelength between 320–370 nm (10-nm intervals). The decay curves were deconvolved in single- and multiple-curve analyses with and without correction for scattered light. In all cases, three exponential functions were required to fit the data and the lifetimes were about 0.5, 2, and 7 ns. Including a term for scattered light in the data anaylsis gave slightly better fits with about the same values for the decay parameters, which authenticates the subnanosecond fluorescence decay. Attempts to fit the data to a four-ex-

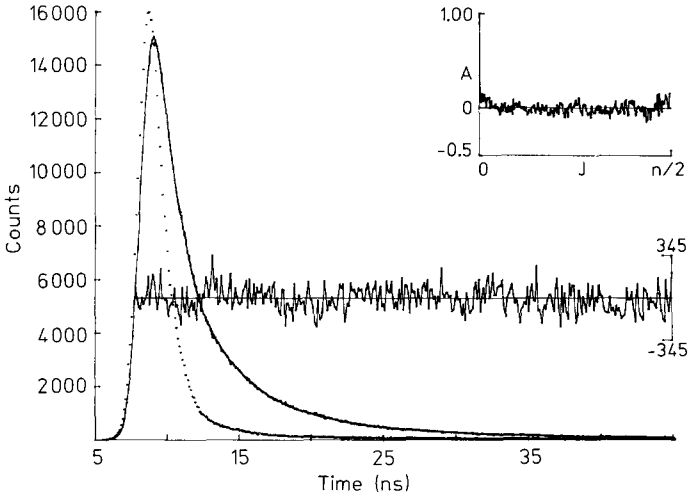

Fig. 4. *Fluorescence decay of high-molecular-mass GB4 glycoform.* Fluorescence decay of fraction 29 from Fig. 2 measured at 295 nm excitation wavelength, 330 nm emission wavelength, 10 °C. The data were fit by global analysis of decay curves at six emission wavelength (320–370 nm, 10-nm intervals) to three exponentials plus a term for scattered light: $\alpha = 0.793$, $\tau_1 = 0.49$ ns, $\alpha_2 = 0.145$, $\tau_2 = 2.63$ ns, $\alpha_3 = 0.041$, $\tau_3 = 7.13$ ns, $a = 0.021$; partial $\chi_r^2 = 0.93$. $\Sigma_i \alpha_i + a = 1$. Right noisy curve: sample decay; left noisy curve: reference decay; smooth curve: best fit to data. The percentage residuals and autocorrelation function (inset) are also shown

Table 2. *Fluorescence decay data of high- and low-molecular-mass GB44 glycoforms*
Results from global analysis of decay curves at six emission wavelengths with scattered light correction

i	τ_i	I_i (at 350 nm)	χ_r^2	$\nu_{cg,i}^{-1}$
	ns			nm
Fraction 29				
1	0.49	0.26	1.07	344
2	2.63	0.36		345
3	7.13	0.37		350
Fraction 37				
1	0.44	0.22	1.14	342
2	2.68	0.12		344
3	7.26	0.12		349

ponential function were unsuccessul. Fig. 4 shows a decay curve for fraction 29 at 330-nm emission wavelength together with the best fit to three exponentials plus scatter obtained by global analysis of the six curves acquired at different emission wavelengths. The global $\chi_r^2 = 1.1$ indicates an excellent fit of the data. However, small nonrandom fluctuations persist in the autocorrelation function (inset), suggesting that the scatter term may represent an unresolved fast exponential decay.

Table 2 summarizes the time-resolved fluorescence data for fractions 29 and 37. The similarity of the lifetime values for the two glycoforms implies that the fluorescence lifetimes of GB44 are not affected by carbohydrate chain length. This conclusion was tested by simultaneous analysis of the decay data for fractions 29 and 37, which constrains the lifetimes for all 12 curves to be the same. The combined 12-curve global analysis gave about the same values for χ_r^2 and the decay parameters as the separate six-curve global analyses.

Table 2 also gives the intensities I_i at 350 nm and the centers of gravity in nm $\nu_{cg,i}^{-1}$ of the emission spectra associated

Table 3. *Acrylamide quenching of high- and low-molecular-mass GB44 glycoforms*
Determined at 295 nm excitation wavelength, 350 nm emission wavelength

Fraction	f_a	K_{sv}	$\langle\tau\rangle$
		M^{-1}	ns
29	0.84	13.9	3.7
37	0.75	13.0	2.8

with the three exponential decays. The intensity of the 0.5-ns component decreased about 15%, whereas the intensities of the 2-ns and 7-ns components decreased about 65% in fraction 37 compared to fraction 29. Such intensity drops in the absence of lifetime drops suggest static quenching of the tryptophan fluorescence in the low-molecular-mass glycoform. The 2-ns and 7-ns components each account for almost 40% of the emission intensity at 350 nm in fraction 29, but less than 30% in fraction 37. The preferential quenching of the longer-lived emission in fraction 37 results in an apparent decrease of about 1 ns in the value of the mean lifetime $\langle\tau\rangle = \Sigma_i f_i(\lambda)\tau_i$ at 350 nm (Table 3). For both fractions 29 and 37, the decay-associated spectra are closely overlapped, with the spectrum of the 7-ns component shifted about 5 nm to the red. This is apparent in the wavelength dependence of the mean lifetime $\langle\tau\rangle$, which increased about 2 ns between 320–370 nm (not shown). Since the centers of gravity of the decay-associated spectra differ little if at all in the two protein fractions, the small blue shift in the steady-state emission spectrum of GB44 with decreasing lactosamine chain length (Fig. 2) is probably due to quenching of the red-shifted emission from the 7-ns component.

Acrylamide quenching

The accessibility of the tryptophan emission in GB44 to small solute molecules was determined by acrylamide quenching experiments. The fluorescence intensity at 350 nm was measured as a function of acrylamide concentration for fractions 29 and 37. The Stern-Volmer plots of the quenching data for both protein fractions showed downward curvature, which suggests that part of the emission is inaccessible to acrylamide (not shown). The modified Stern-Volmer plots were linear (Fig. 5). The values of the quenching parameters are given in Table 3. The fraction of emission accessible to acrylamide f_a was roughly the same in the two protein samples, despite the fact that 50% of the fluorescence intensity of fraction 29 is absent in fraction 37. This suggests that the drop in fluorescence intensity of GB44 with decreasing lactosamine chain length involves both exposed and buried tryptophans. The Stern-Volmer constant K_{sv} for the accessible emission is likewise about the same in the two protein fractions. In proteins with multiple tryptophans, the apparent Stern-Volmer constant derived from the modified plot is a complicated function of the quenching constants $K_{sv,j}$ for individual residues. At low concentrations of quencher the inverse slope $f_a K_{sv}$ of the modified plot is equal to the effective Stern-Volmer constant $K_{sv}(\text{eff}) = \Sigma_j f_j K_{sv,j}$, where f_j is the fractional intensity of tryptophan j [31]. In the absence of static quenching, the individual Stern-Volmer constants are $K_{sv,j} = k_{q,j}\tau_j$, where $k_{q,j}$ is the collisional quenching rate constant and τ_j is the fluorescence lifetime in the absence of quencher. Assuming that $K_{sv}(\text{eff}) \approx k_q(\text{app})\langle\tau\rangle$, we estimate an apparent quench-

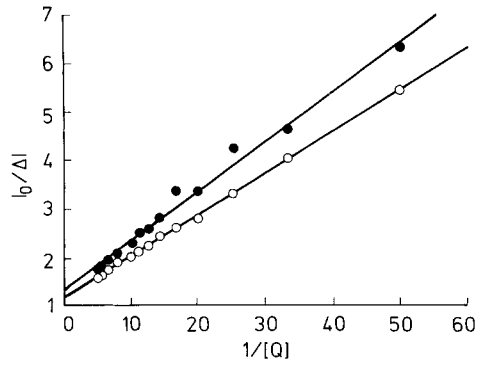

Fig. 5. *Modified Stern-Volmer plots of acrylamide quenching data of high- and low-molecular-mass GB44 glycoforms.* Measured at 295 nm excitation wavelength, 350 nm emission wavelenght, 22 °C: (○) fraction 29 and (●) fraction 37

ing rate constant of about 3×10^9 M^{-1} s^{-1} for both fractions 29 and 37. This high value indicates that the accessible tryptophans in GB44 are on the surface of the glycoprotein [32].

Anisotropy

The fluorescence emission anisotropy of GB44 increased with decreasing lactosamine chain length (Table 1). The relative changes in the anisotropy values were about the same at 350 nm and 370 nm emission wavelength (not shown), indicating they are not due to light scattering in the more weakly fluorescent fractions. The steady-state anisotropy $\langle r \rangle$ depends on the ratio of the fluorescence lifetime τ and the rotational correlation time ϕ. For isotropic rotation of a rigid fluorophore with a single lifetime

$$\langle r \rangle = r_o/(1 + \tau/\phi),$$

where r_o is the limiting anisotropy in a frozen solution. Typical r_o values for tryptophan in proteins are 0.17–0.19 at 295 nm excitation wavelength [3]. Substituting these r_o values and the mean lifetime $\langle \tau \rangle$ into the above equation gives a crude estimate of the apparent rotational correlation time of GB44: $\phi = 2.1-2.5$ ns for fraction 29 and $\phi = 9-16$ ns for fraction 37. The rotational correlation time of a sphere is $\phi = V_h\eta/kT$, where V_h is its hydrodynamic volume, η is solvent viscosity, k is the Boltzmann constant, and T is absolute temperature. For globular proteins of 40–60 kDa, the expected rotational correlation times in aqueous solution at 22 °C are about 16–23 ns. The value of about 2 ns estimated for fraction 29 suggests that the fluorescent tryptophans have greater internal mobility in the high-molecular-mass glycoform than in the low-molecular-mass glycoform.

DISCUSSION

We have compared the intrinsic tryptophan fluorescence of a series of polylactosamine glycoforms of the gelatin-binding domain GB44 of human placental fibronectin. GB44 glycoforms with high amounts of polylactosamine on the three N-linked carbohydrate chains had greater fluorescence intensity, red-shifted emission spectra, and lower anisotropy values. However, the fluorescence lifetimes and accessibility to solute quencher were essentially the same in high- and low-molecular-mass GB44 glycoforms. The fluorescence intensity and anisotropy changes and the emission spectral shifts report differences in the tryptophan environments of GB44 in the various glycoforms. These could be due to changes in the protein conformation or in the interactions between surface tryptophans and the carbohydrate chains. The gelatin-binding domain of fibronectin has nine tryptophans in its 340-amino-acid sequence [34]. The presence of multiple tryptophans in GB44 complicates interpretation of the fluorescence results. The tryptophans are located at positions 291, 354, 414, 453, 475, 522, 545, 566, and 599. Eight of them occur in the four type-I and two type-II homology units and one is at the C-terminus. There are two disulfide bridges in each of the six homology units. Five of the tryptophans are one or two residues away from disulfides, which quench tryptophan fluorescence [35]. Isaacs et al. [30] showed that the unusually low quantum yield of the plasma glycoform is due in part to the disulfides.

The decrease in tryptophan fluorescence of GB44 with decreasing carbohydrate chain length could be caused by static and dynamic quenching processes. Static quenching is due to formation of nonfluorescent ground-state complexes. These could arise in GB44 from interactions between tryptophans and carbohydrate as well as polypeptide functional groups. Dynamic quenching is due to competing nonradiative pathway for deactivation of the excited state, such as collisional quenching, excited-state reactions, and energy transfer. Diffusive motion of the carbohydrate chains of GB44 might quench the fluorescence of surface tryptophans. Tryptophan itself is susceptible to dynamic quenching by excited-state proton and electron transfer reactions [36]. In GB44, quenching reactions involving tryptophan and functional groups on the polypeptide or the carbohydrate may occur. Potential quenching groups on the polylactosamine chains are the carbonyl groups of the internal *N*-acetylglucosamine and the terminal sialic acids. Alcoholic hydroxyl groups do not quench the fluorescence of the indole chromophore [37]. Finally, tryptophan–tryptophan energy transfer appears to occur in other multitryptophan proteins [38, 39]. In principle, fluorescence decay measurements can distinguish static (amplitude drops) and dynamic (lifetime drops) quenching. We have resolved the fluorescence decay of GB44 into three exponential components and have found no evidence for lifetime decreases in the low-molecular-mass glycoform. The three exponential decays of about 0.5, 2, and 7 ns represent an empirical fit of the data. Even single tryptophans in proteins typically exhibit complex fluorescence decays [40] comprised of discrete lifetimes or continuous lifetime distributions [41]. With only partial resolution of the fluorescence decay of GB44, it is impossible to exclude lifetime drops in which emission has transferred from a longer to a shorter lifetime component. However, the emission of all three lifetime components was quenched in the low-molecular-mass glycoform with no significant shifts in the decay-associated spectra. Thus, static quenching appears to be a reasonable explanation of the decrease in fluorescence intensity of GB44 with decreasing polylactosamine chain length.

The fluorescence lifetimes also help clarify the solute quenching and anisotropy results. In multitryptophan proteins the apparent steady-state values are complicated functions of the parameters for individual tryptophans. We have used the mean lifetime values to estimate apparent values of the quenching rate constants and rotational correlation times. The time-resolved measurements were performed at lower temperature (10 °C compared to 22 °C) to preserve the protein samples during the long data acquisitions. The fluorescence intensity of GB44 does not vary dramatically in this tempera-

ture region, so we do not expect the mean lifetimes to be highly temperature-dependent. The apparent values of the quenching rate constants and rotational correlation times are useful for qualitative comparisons of the high- and low-molecular-mass glycoforms of GB44. However, the conclusions are not definitive, because the populations of fluorescent tryptophans may not be the same in the two glycoproteins. Nevertheless, the value of about $3 \times 10^9\ M^{-1}s^{-1}$ for the quenching rate constant indicates that the solute-accessible emission in GB44 comes from surface tryptophans. The polylactosamine chains do not appear to interfere with acrylamide quenching of surface tryptophans in either the high- or low-molecular-mass glycoforms. The low apparent values of the correlation times indicate internal motions of the tryptophans in GB44. The tryptophan environments appear to become more rigid with decreasing polylactosamine chain length.

The fluorescence results are consistent with glycosylation-dependent changes in protein conformation. The polar emission maxima and large solute quenching rate constants argue that most of the fluorescence in GB44 is due to surface tryptophans exposed to solvent. Our tentative explanation for the effects of carbohydrate chain length is a mechanical model, in which the highly solvated polylactosamine chains diffusing in solution tug on the protein surface. We image that this would loosen the surface structure and reduce amino acid side-chain contacts, thereby increasing the motional freedom of surface tryptophans and relieving static quenching of their fluorescence. An alternative explanation would be that the polylactosamine chains lie along the protein surface and perturb the protein structure. NMR studies of the solution conformation of N-linked oligosaccharides showed that the six-arm in complex structures can fold back over the mannose core [42]. Low-angle neutron and X-ray scattering studies of th α_1-acid glycoprotein glycoforms revealed two modes of protein–carbohydrate interactions in the single lactosamine-type complex chains [17]. The biantennary chains were loosely bound to the protein surface, while the tri- and tetraantennary chains were tightly anchored through their sialic acid termini. Although we cannot exclude the possibility of tryptophan–carbohydrate interactions in the GB44 glycoforms, we tend to discount this interpretation of the fluorescence results on two grounds. First, the tryptophans are spaced about 20–60 residues apart throughout the peptide sequence. We would expect that the longer polylactosamine chains would have more opportunity to interact with surface tryptophans and quench their fluorescence, which is opposite to our findings. And second, the most likely quenching agent on the carbohydrate is the carbonyl group of the *N*-acetylglucosamines and sialic acids. However, the greatest quenching is observed when the carbohydrate is trimmed close to the mannose core by endo-β-galactosidase.

The GB44 glycoforms used in this investigation are mixtures which have been fractionated on the basis of size. It is not possible with current technology to separate the polylactosamine series into individual molecular idiotypes. The fractions from gel permeation chromatography represent relatively narrow distributions of glycoforms with reproducible centroids. The heterogeneity within a given fraction consists mainly in the degree of polymerization of lactosamine subunits on the arms of N-linked tetraantennary chains. The three glycosylated asparagines in the gelatin-binding domain of fibronectin are located at positions 399, 497, and 511 [34]. An average of two of these sites are occupied in the chymotryptic gelatin-binding fragment from plasma, while all three glycosylation sites are occupied in the analogous fragment from placenta [4]. The plasma glycoform has only biantennary chains, whereas the placental glycoforms have about 30% biantennary, no triantennary, and 70% tetra-antennary carbohydrate [22]. Since none of the glycosylation sites are adjacent to tryptophans, we consider the aggregate effect of the lactosamine subunits to be responsible for the observed differences in the tryptophan fluorescence of the GB44 glycoforms. Although carbohydrate sequence-specific effects may play a role, we favor the notion that the length of the polylactosamine chains is the important variable in this system. In this regard we note that the largest fluorescence changes occur when the apparent molecular mass increases from 52 kDa to 58 kDa (with carbohydrate increasing from about 17 kDa to 23 kDa), suggesting a threshold phenomenon.

In conclusion, our data show that polylactosamine glycosylation on N-linked chains increases the fluorescence quantum yield of tryptophans in the gelatin-binding domain from fetal tissue fibronectin. The effect can be reversed by removal of the lactosamine oligomers. These long-chain oligosaccharides, which have been shown to inhibit both proteolysis and gelatin-binding of this polypeptide, apparently change the conformation of the protein as manifested by changes in the quantum yield and emission anisotropy of the intrinsic tryptophans. The results reported here give the first evidence that polylactosamine elongation of N-linked complex saccharides can incrementally alter protein conformation. This suggests that the observed functional differences [4, 12, 22] in various glycoforms of fibronectin and its specific binding domains may be caused not only by steric interference with binding sites, but by subtle changes in the protein structure. Thus, organisms have another mechanism to control functions of a single polypeptide gene product by post-translational modification.

This work was supported by National Institutes of Health Grants GM32594 to R. A. L. and GM35009 to M. D. B.

REFERENCES

1. Pazur, J. H., Knull, H. R. & Simpson, D. L. (1970) *Biochem. Biophys. Res. Commun. 40*, 110–116.
2. Kornfeld, S. (1985) *Annu. Rev. Biochem. 54*, 631–664.
3. Peterson, C. B. & Blackburn, M. N. (1985) *J. Biol. Chem. 260*, 610–615.
4. Zhu, B. C. R. & Laine, R. A. (1985) *J. Biol. Chem. 60*, 4041–4045.
5. Rademacher, T. W., Parekh, R. B. & Dwek, R. A. (1988) *Annu. Rev. Biochem. 57*, 785–838.
6. Chu, F. K., Trimble, R. B. & Maley, F. (1978) *J. Biol. Chem. 253*, 8691–8693.
7. Cheng, S.-Y., Morrone, S. & Robbins, J. (1979) *J. Biol. Chem. 254*, 8830–8835.
8. Shifrin, S., Consiglio, E., Laccetti, P., Salvatore, G. & Kohn, L. D. (1982) *J. Biol. Chem. 257*, 9539–9547.
9. Shifrin, S., Consiglio, E. & Kohn, L. D. (1983) *J. Biol. Chem. 258*, 3780–3786.
10. Grimaldi, S., Robbins, J. & Edelhoch, H. (1985) *Biochemistry 24*, 3771–3776.
11. Keutmann, H. T., Johnson, L. & Ryan, R. J. (1985) FEBS Lett. 185, 333–338.
12. Jones, G. E., Arumugham, R. G. & Tanzer, M. L. (1986) *J. Cell Biol. 103*, 1663–1670.
13. Basu, S., Mandal, C. & Allen, A. K. (1988) *Biochem. J. 254*, 195–202.
14. Sakiyama, H., Matsushita, E., Kuwabara, I., Nozue, M., Takahashi, T. & Taniguchi, M. (1988) *Cancer Res. 48*, 7173–7178.

15. Seidel-Dugan, C., Ponce de Leon, M., Friedman, H. M., Fries, L. F., Frank, M. M., Cohen, G. H. & Eisenberg, R. J. (1988) *J. Virol. 62*, 4027–4036.
16. Bayard, B. & Kerckaert, J.-P. (1980) *Biochem. Biophys. Res. Commun. 95*, 777–784.
17. Perkins, S. J., Kerckaert, J.-P. & Loucheux-Lefebvre, M. H. (1985) *Eur. J. Biochem. 147*, 525–531.
18. Hoffman, S., Sorkin, B. C., Perrin, W. C., Brackenberry, R., Mailhammer, R., Rutishauser, U., Cunningham, B. A. & Edelman, G. M. (1982) *J. Biol. Chem. 257*, 7720–7729.
19. Finne, J., Finne, U., Deagostini-Bazin, H. & Goridis, C. (1983) *Biochem. Biophys. Res. Commun. 112*, 482–487.
20. Hoffman, S. & Edelman, G. M. (1983) *Proc. Natl Acad. Sci. USA 80*, 5762–5766.
21. Zhu, B. C. R. & Laine, R. A. (1987) *Arch. Biochem. Biophys. 252*, 1–6.
22. Zhu, B. C. R., Fisher, S. F., Pande, H., Calaycay, J., Shively, J. E. & Laine, R. A. (1984) *J. Biol. Chem. 259*, 3962–3970.
23. Sairam, M. R. & Manjunath, P. (1982) *Int. J. Peptide Protein Res. 19*, 315–320.
24. Knudsen, K. A. (1985) *J. Cell. Biol. 101*, 891–897.
25. Melhuish, W. H. (1961) *J. Phys. Chem. 65*, 229–235.
26. Kolber, Z. S. & Barkley, M. D. (1986) *Anal. Biochem. 152*, 6–21.
27. Knutson, J. R., Beechem, J. M. & Brand, L. (1983) *Chem. Phys. Lett. 102*, 501–507.
28. Lakowicz, J. R. & Hogen, D. (1981) *Biochemistry 20*, 1366–1373.
29. Sun, M. & Song, P.-S. (1977) *Photochem. Photobiol. 25*, 3–9.
30. Isaacs, B. S., Brew, S. A. & Ingham, K. C. (1989) *Biochemistry 28*, 842–850.
31. Lehrer, S. S. & Leavis, P. C. (1978) *Methods Enzymol. 49*, 222–236.
32. Eftink, M. R. & Ghiron, C. A. (1981) *Anal. Biochem. 114*, 199–227.
33. Lakowicz, J. R., Maliwal, B. P., Cherek, H. & Balter, A. (1983) *Biochemistry 22*, 1741–1752.
34. Skorstengaard, K., Jensen, M. S., Sahl, P., Petersen, T. E. & Magnusson, S. (1986) *Eur. J. Biochem. 61*, 441–453.
35. Cowgill, R. W. (1967) *Biochim. Biophys. Acta 140*, 37–44.
36. Creed, D. (1984) *Photochem. Photobiol. 39*, 537–562.
37. Feitelson, J. (1970) *Israel J. Chem 8*, 241–252.
38. Desie, G., Boens, N. & De Schryver, F. C. (1986) *Biochemistry 25*, 8301–8308.
39. Eftink, M. R., Wasylewski, Z. & Ghiron, C. A. (1987) *Biochemistry 26*, 8338–8346.
40. Beechem, J. M. & Brand, L. (1985) *Annu. Rev. Biochem. 54*, 43–71.
41. Alcala, J. R., Gratton, E. & Prendergast, F. G. (1987) *Biophys. J. 51*, 597–604.
42. Brisson, J.-R. & Carver, J. P. (1983) *Biochemistry 22*, 3680–3686.